JOURNAL OF MATERIALS SCIENCE 30 (1995) 3633–3638

Ion transport studies in PEO: NH_4I polymer electrolytes with dispersed Al_2O_3

A. CHANDRA, P.C. SRIVASTAVA, S. CHANDRA*
Physics Department, Banaras Hindu University, Varanasi 221005, India

Ion conducting polymer electrolyte films having high salt concentrations have been studied. The system studied is PEO: NH_4I, dispersed with α-Al_2O_3. Mechanically stable films with NH_4^+/EO ratio ≥ 0.13 have been obtained by dispersal of Al_2O_3. The films have been characterized using various techniques such as X-ray diffraction (XRD), differential thermal analysis (DTA), polarization and complex impedance spectroscopy. Intercorrelation between polymer matrix crystallite size, conductivity, and α-Al_2O_3 particle size is established.

1. Introduction

Some of the PEO based polymer electrolytes are limited by poor mechanical properties, in spite of their reasonably high electrical conductivity and thereby the possibility of their use in a large number of practical applications. Recently, it has been realised that developing proton (H^+) conductors have vast technological applications, particularly in fuel cells and sensors. Some of the reported PEO based proton conductors are, PEO: NH_4SCN, PEO: $NH_4SO_3CF_3$ [1], PEO: NH_4HSO_4 [2], PEO: NH_4ClO_4 [3,4], PEO: H_3PO_4 [5], PEO: $(NH_4)_2SO_4$ [6], PEO: NH_4I [7].

For most polymer electrolytes the conductivity decreases at higher concentrations due to ion-association. However, Maurya *et al.* [7] have reported in their studies on the PEO: NH_4I system that its conductivity keeps on increasing until 70:30 wt% ratio is reached. Beyond this weight percent ratio (NH_4/EO ≥ 0.13), the films become mechanically unstable and "glue-like". The motivation of this study was to prepare mechanically stable films (i.e. films which could be handled with ease and were non-sticky) with higher NH_4I content in PEO with the hope that a higher conductivity will be obtained. To achieve this goal, we dispersed α-Al_2O_3 in PEO and studied the following:

(i) Differential thermal analysis (DTA) for obtaining phase diagrams.
(ii) X-ray diffraction (XRD) for d-values and crystallite size.
(iii) σ versus Al_2O_3 content for different films.
(iv) σ versus Al_2O_3 particle size.
(v) Correlation between σ and polymer matrix crystallite size (i.e. Scherrer length).
(vi) σ versus $1/T$ for different films.

We have found that Al_2O_3 forms a dispersed phase system with the polymer electrolyte and also affects the crystallinity (and hence the conductivity) of the polymer electrolyte.

2. Experimental procedure

The experimental methods used to obtain and characterize the PEO: NH_4I (+ Al_2O_3) polymer films are given below:

2.1. Film preparation

Polymer films were prepared by the well known solution cast technique. PEO (MW = 6×10^5) and NH_4I were weighed for different NH_4^+/EO ratios (0.034, 0.076, 0.13, 0.20, 0.30) and were dissolved in distilled methanol. To this mixture Al_2O_3 was added in different weight percentages (1, 5, 10, 15, 20, 30, 40, 50) and the solution was stirred for ~8–10 h at 40 °C. The highly viscous solutions thus obtained were poured into polypropylene dishes and the solvent was allowed to evaporate in dry ambient air. These films were then vacuum dried at ~0.013 Pa for 24 h to remove traces of solvent. Aluminium was vacuum coated onto both sides of the films (using masks of known area) to take electrical contacts.

2.2. Complex impedance plots

Complex impedance plots of PEO: NH_4I (+ Al_2O_3) polymer films were obtained using a Solartron (1250 frequency response analyser and 1286 electrochemical interface) coupled to a HP-computer. The measurements were taken in the frequency range 6.5Hz–65 KHz.

2.3. X-ray diffraction

XRD patterns of the polymer films were taken on a Rigaku Rotaflex unit with scan speed of $2°\,min^{-1}$. The size of the PEO crystallites (L) have been calculated using the Scherrer formula, given as

$$L = \frac{0.9\lambda}{B\cos\theta_B} \quad (1)$$

* Author to whom all correspondence is to be addressed.

0022–2461

where λ is the wavelength of the X-rays used, B is the full width at half maximum intensity (in radians) of the XRD peak at θ_B.

2.4. Differential thermal analysis

DTA of the PEO: NH_4I (+ Al_2O_3) films was carried out with a Linseis's unit (Model 2045). The measurements were done from room temperature (~ 30 °C) to 200 °C at a heating rate of 5 °C min^{-1}.

2.5. Ionic transference number

Wagner's polarization method was used to find out the total ionic transference number. The polarization was performed by applying a d.c. bias of 200 mV and the current was measured by a Keithley source measure unit (Model 236).

3. Results and discussion

The structural and ion transport studies carried out on the PEO: NH_4I (+ Al_2O_3) systems are given below.

3.1. Differential thermal analysis (DTA)

DTA is reported by Maurya *et al.* [7] for PEO: NH_4I for different NH_4^+/EO ratios but with no alumina. Here, we wanted to study the effect (if any) caused in the phase diagram of PEO: NH_4I on the dispersal of Al_2O_3. Therefore, DTA was carried out for PEO: NH_4I films with NH_4^+/EO = 0.13 with 0, 1, 10, 20, 30, 40 and 50 wt% of Al_2O_3. The results are shown in Fig. 1. A comparison of all the DTA curves shows that the dispersal of Al_2O_3 introduces only the following minor changes:

(a) The PEO: NH_4I complex T_m "peak" corresponding to melting of PEO in the crystalline phase, at 66°C for a sample with no Al_2O_3, shifts slightly to the lower temperature side by ≤ 3 °C as Al_2O_3 content is increased.

(b) The broad peak at ~86 °C in 0% Al_2O_3 film (identified as T_m for the crystalline complex of PEO, abbreviated as $(PEO)_{cc}$, splits into two peaks. The split peak (at ~78 °C) on the lower side of the original peak (at 86 °C) shows a similar shift to T_m (66 °C) given above with the addition of Al_2O_3. The other split peak is tentatively assigned to $(PEO)_{cc,Al_2O_3}$ assuming that the Al_2O_3 dispersal affects the energetics of $(PEO)_{cc}$ by distorting the PEO helical chain.

Fig. 2 is the phase diagram of the PEO: NH_4I polymer film (NH_4^+/EO = 0.13) based on DTA curves for different weight percentages of Al_2O_3 given in Fig. 1. In this figure, Region I is marked by the coexistence of PEO in the crystalline form $(PEO)_c$, PEO in the crystalline complex form $(PEO)_{cc}$, and PEO crystalline complex distorted due to Al_2O_3 $(PEO)_{cc,Al_2O_3}$, Region II contains the $(PEO)_{cc}$ and $(PEO)_{cc,Al_2O_3}$. Region III has only the $(PEO)_{cc,Al_2O_3}$. Region IV is the liquidus phase.

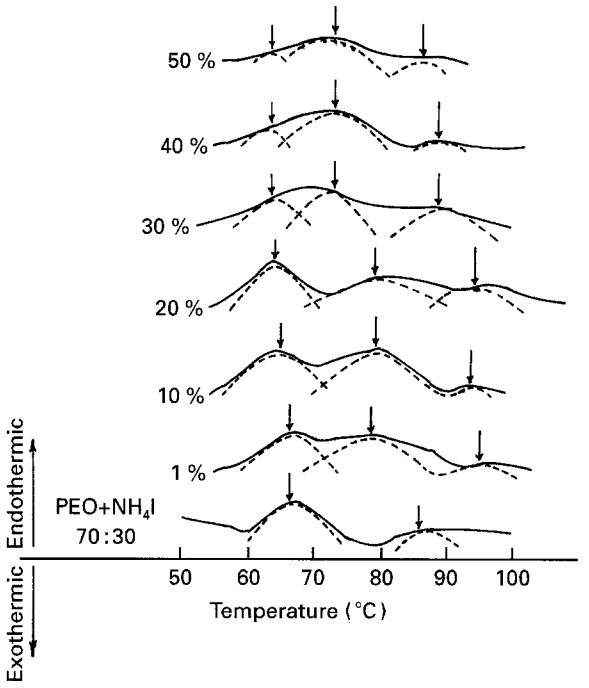

Figure 1 DTA curves for PEO: NH_4I (+ Al_2O_3) films with different wt % of α-Al_2O_3 (< 10μm).

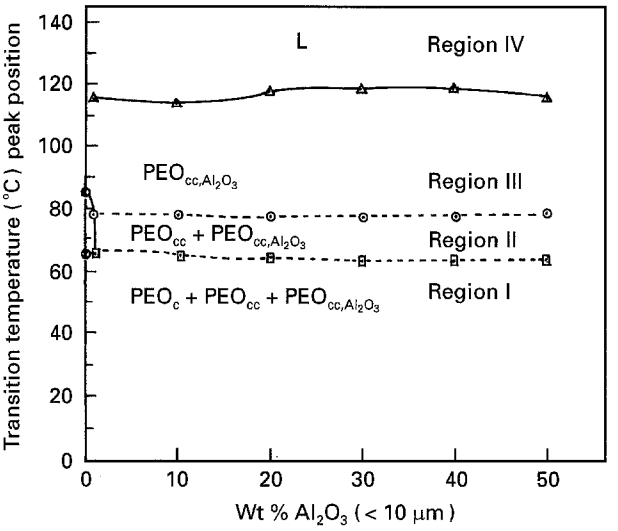

Figure 2 Phase diagram for PEO: NH_4I (+ Al_2O_3).

3.2. X-Ray diffraction

In PEO: NH_4I films without Al_2O_3, it is observed that for NH_4^+/EO ratio equal to 0.13, there are no well-defined peaks. Instead there are a few overlapping peaks indicative of a low degree of crystallinity. Fig. 3 gives the XRD patterns of PEO: NH_4I films (with NH_4^+/EO = 0.13) with 0, 10, 20 and 50 wt% of α-Al_2O_3. From these figures it is obvious that an addition of α-Al_2O_3 increases the crystallinity in the otherwise low crystallinity films. From this figure it is also clear that the addition of α-Al_2O_3 modifies the lattice, changing the "d" and 2θ values. The shifts in "d" and 2θ values are given in Table I. It may be remarked here that the enhancement in the crystallinity (and changes in "d-values") are likely to affect the conductivity of these films (actually found by us and discussed later). Further, it should also be noted that α-Al_2O_3 is forming a dispersed phase with PEO:

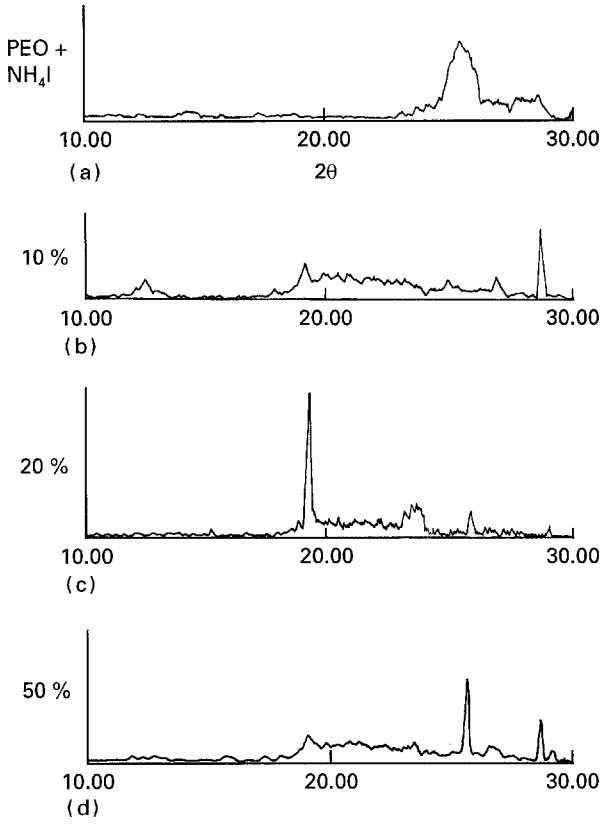

Figure 3 XRD patterns of PEO: NH_4I (+ Al_2O_3) films with different wt % of Al_2O_3 (< 10μm).

TABLE I Changes in "d" and 2θ values due to dispersal of α-Al_2O_3 in PEO: NH_4I films (NH_4^+/EO = 0.13)

d-values for films with Al_2O_3 wt %			2θ ° for films with Al_2O_3 wt %		
10%	20%	50%	10%	20%	50%
7.07	–	–	12.5	–	–
	4.71	–	–	18.71	–
4.63	4.61	4.62	19.14	19.21	19.19
	3.78	3.76	–	23.5	23.58
3.57	3.46	3.46	24.91	25.67	25.72
3.30	–	3.32	26.92	–	26.76
3.10	3.11	3.10	28.75	28.79	28.77

NH_4I system as characteristic reflections of α-Al_2O_3 were found to be present in the XRD patterns.

3.3. Ionic transference number

The ionic transference number for the films with different wt% of Al_2O_3 has been determined using the Wagner's polarization method. The cell configuration used is

$$Al|PEO: NH_4I + (Al_2O_3)|Al \qquad (2)$$

A d.c. bias of 200 mV has been applied across the cell and the current has been monitored with time. Two typical plots between time and current are shown in Fig. 4 for PEO: NH_4I: + Al_2O_3 films with NH_4^+/EO = 0.13; alumina contents 5 wt% (curve (a)) and 30 wt% (curve (b)). The corresponding values of t_{ion} are 0.99 and 0.97. The ionic transference number

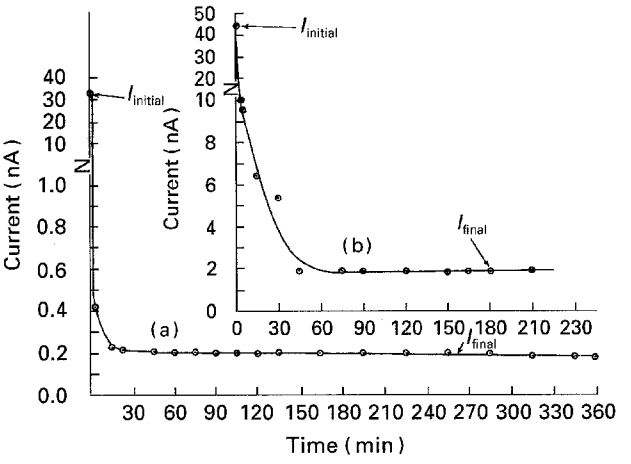

Figure 4 d.c. polarization (Wagner's polarization) curves for (a) PEO: NH_4I (+ Al_2O_3), NH_4^+/EO = 0.13, 5wt% α-Al_2O_3, t_{ion} = 0.99. (b) PEO: NH_4I (+ Al_2O_3), NH_4^+/EO = 0.13, 30 wt % α-Al_2O_3, t_{ion} = 0.97.

(t_{ion}) has been calculated employing the relation

$$t_{ion} = \frac{I_{initial} - I_{final}}{I_{initial}} \qquad (3)$$

where $I_{initial}$ and I_{final} are the total initial and the final residual current respectively.

3.4. Dependence of conductivity on Al_2O_3 content

The bulk electrical conductivity was evaluated by complex impedance/admittance plots. Films for five different weight percentages of NH_4I in PEO (NH_4^+/EO = 0.034, 0.076, 0.13, 0.2 and 0.3) were prepared. In each of these compositions, different weight percentages of α-Al_2O_3 was dispersed (1, 5, 10, 20, 30, 40 wt%). Two temperatures (70 °C and 100 °C) were chosen for this study. Fig. 5(a) and (b) show the variation of bulk conductivity with wt% of Al_2O_3 for different NH_4^+/EO ratios at 70 °C and 100°C, respectively. In these figures it is seen that there is a broad minimum in each σ versus % Al_2O_3 curve, approximately corresponding to 10–30 wt% value of Al_2O_3 content. The variation in conductivity is possibly related to the fact that the materials are dispersed phase systems and their crystallinity changes. The correlation between crystallinity and conductivity is discussed later in this paper.

3.5. Dependence of conductivity on Al_2O_3 particle size

Several workers [8, 9] have reported that the size of the particle dispersed has a significant role in the change of conductivity. Fig. 6 shows the effect of dispersoid particle size on conductivity for the films of the same composition; (NH_4^+/EO = 0.13), 20 wt% of Al_2O_3. Conductivity isotherms at 60 and 110 °C are shown in Fig. 7. It is obvious that (a) conductivity enhancement is higher for smaller particle size (100 μm ≤ 38 μm ≤ 10 μm, and (b) particle size effect is more pronounced below T_m(~60 °C) than above T_m(~110 °C). The conclusion (a) has been drawn by

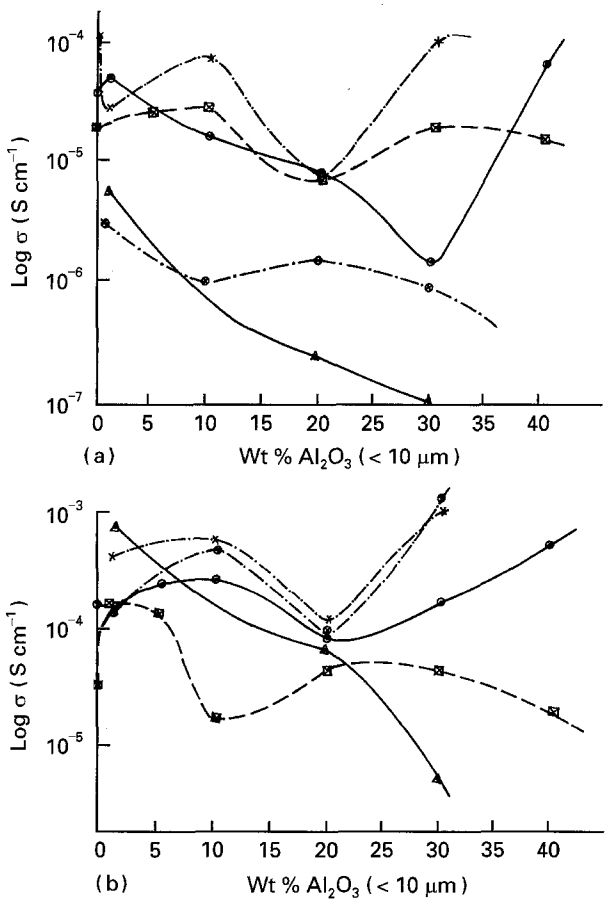

Figure 5 Variation of conductivity with wt % of α-Al_2O_3 for films with different NH_4^+/EO ratios at (a) 70 °C and (b) 100 °C. Ratios: ⊙ 0.034; ⊠ 0.076; × 0.13; ⊗ 0.2; △0.3.

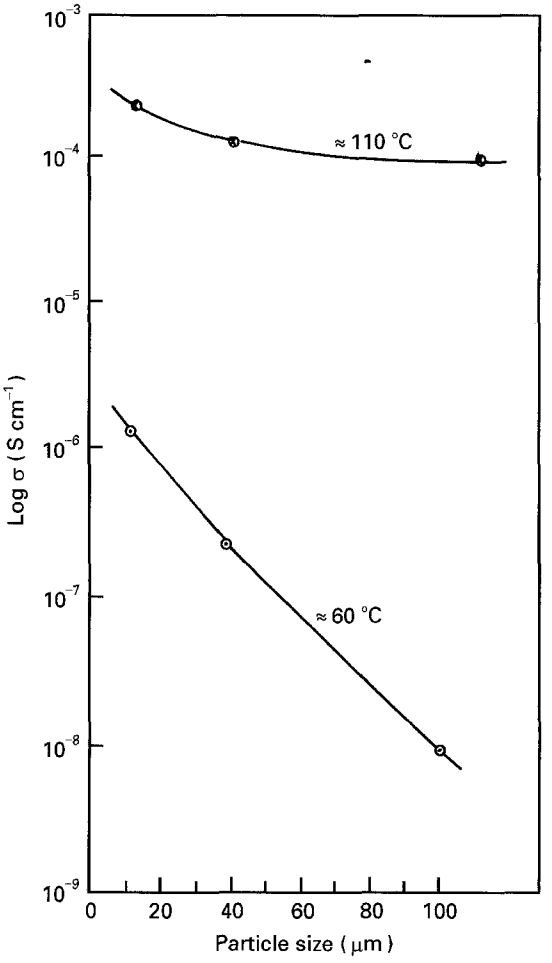

Figure 7 Conductivity isotherms exhibiting the effect of dispersoid particle size at ~60 °C (below T_m) ⊙ and ~110 °C (above T_m) (⊗).

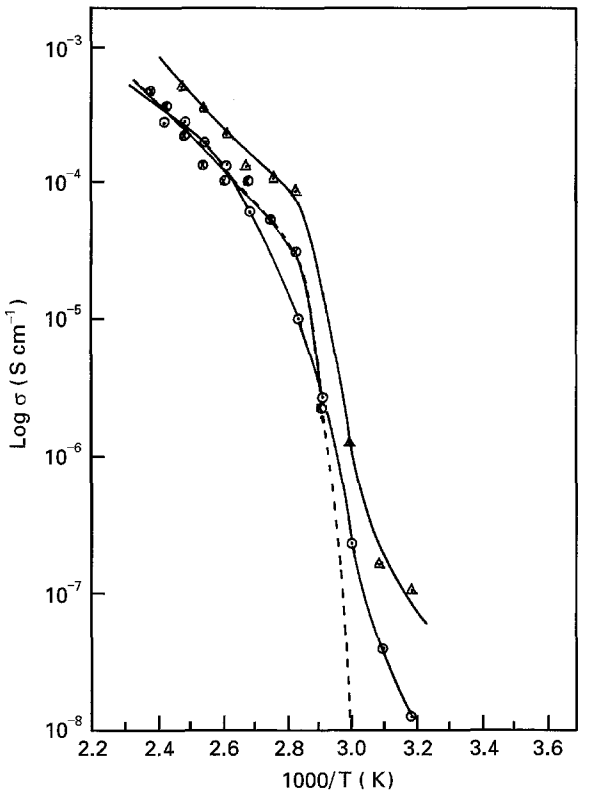

Figure 6 Temperature dependence of conductivity for three films with different particle sizes of the dispersed α-Al_2O_3. The composition of PEO: NH_4I (+ Al_2O_3) films is NH_4^+/EO = 0.13, with 20 wt % of α-Al_2O_3. △ ≤ 10 μm; ⊙ ≤ 38μm; ⊗ ≤ 100 μm.

earlier workers on many dispersed phase systems and explained on the basis of relative grain boundary region and percolation difficulties. Above melting temperature T_m, the host PEO matrix is amorphous and the intergrain connection can be obtained with greater ease, and hence, the particle size effect is not shown up prominently.

3.6. Correlation between σ and polymer matrix crystallite size (Scherrer length)

The dispersal of Al_2O_3 is expected to change the crystallinity of the sample which subsequently would effect the conductivity. An indirect method of estimating crystallinity is to determine the linewidth of XRD peaks of PEO. We have chosen three prominent PEO peaks from the XRD pattern given earlier in Fig. 3 at $2\theta = 19\,°(\pm 0.5°)$, $24\,°(\pm 1\,°)$ and $28\,°(\pm 1\,°)$ for XRD linewidth measurements. The measured linewidths are given in Table II. The calculated values of L with wt% of Al_2O_3 is given in Table II. The variation of Scherrer length with alumina content is shown in Fig. 8(a). The variation of conductivity versus wt% Al_2O_3 is shown in Fig. 8(b). It is obvious that there exists a correlation between Scherrer length and σ. As the crystallite size (L) increases, the conductivity decreases. Hence, it can be said that, conductivity in PEO: NH_4I (+ Al_2O_3) system is greatly influenced by the wt% of dispersoid through a consequential change in the crystallite size of the host matrix.

TABLE II Calculated Scherrer length (L) and change in XRD linewidth of three prominent peaks for PEO: NH_4I (70: 30) films with different amounts of α-Al_2O_3

Peak position ($2\theta_B$)	Measured linewidth for films with Al_2O_3 wt %			L (nm) for films with Al_2O_3 wt %		
	10%	20%	50%	10%	20%	50%
19°(±0.5)°	0.45°	0.27°	0.465°	17.9	29.8	17.3
24°(±1)°	0.33°	0.27°	0.405°	24.6	30.2	23.5
28°(±1)°	0.40°	0.3°	0.39°	20.1	27.5	23.6

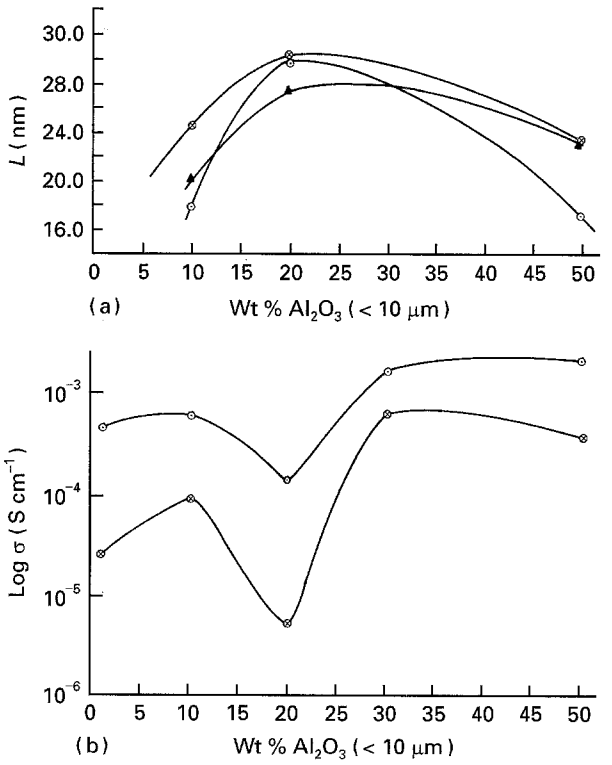

Figure 8 (a) Variation of PEO matrix crystallite size (Scherrer length, L) with wt % of α-Al_2O_3, ⊗ $2\theta \approx 24°(\pm 1°)$ peak; $\Delta 2\theta \approx 27°(\pm 1°)$ peak; ⊙$2\theta \approx 19°(\pm 0.5°)$ peak; (b) Variation of conductivity with wt % of α-Al_2O_3 at 70 °C (⊗) and 100 °C (⊙).

3.7. Temperature dependence of conductivity

Fig. 9 shows the temperature dependence of conductivity for films with NH_4^+/EO ratio equal to 0.13 with different weight percentages of Al_2O_3 dispersed in them. Two "apparent" Arrhenius type

$$\sigma = \sigma_0 \exp(-E_a/kT) \quad (4)$$

linear regions can be identified in the $\log \sigma$ versus $1/T$ plots: one for temperatures $T > T_m$ and the other for $T < T_m$. The conductivity changes on the addition of Al_2O_3 are more evident at $T < T_m$ while for $T > T_m$ the changes are relatively less. Mechanically good films with best conductivity are those for which NH_4/EO = 0.13, 5 wt% Al_2O_3 and NH_4^+/EO = 0.2, 30% of Al_2O_3. The values of σ_0 for these films respectively are: 3.1×10^2 S cm^{-1} and 1.83×10^1 S cm^{-1} while the values of E_a are 0.43 eV and 0.38 eV. A general conclusion (Poulsen *et al.* [10]) that higher conductivity is associated with a higher value of σ_0 and lower

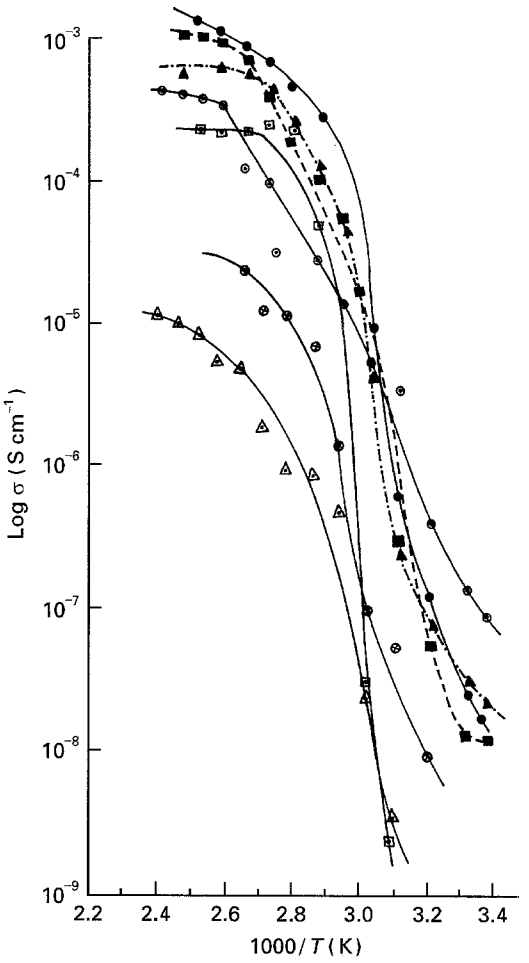

Figure 9 σ versus $1000/T$ plots for NH_4^+/EO = 0.13, with different wt % α-Al_2O_3; ● 0; ⊙ 1; ■ 5; △10; ⊡15; ▲ 30; ⊗ 50.

TABLE III The values of pre-exponential factor σ_0 and activation energy E_a above T_m evaluated from ln σ versus $1/T$ plot for PEO: NH_4I films (NH_4^+/EO = 0.13) with different wt % of Al_2O_3

wt % Al_2O_3	σ_0 (S cm^{-1})	E_a (eV)
1	4.2×10^{-3}	0.08
5	3.07×10^2	0.43
10	6.12×10^{-3}	0.23

E_a is also borne out by our results. Typical values of σ_0 and E_a for one of the best films (i.e. NH_4^+/EO = 0.13 film) with different wt% of alumina are given in Table III.

4. Conclusions

XRD, DTA, σ versus $1/T$, σ versus Al_2O_3 content and σ versus Al_2O_3 particle size have been studied for PEO: NH_4I films of many NH_4^+/EO ratios in which different amounts of α-Al_2O_3 were dispersed. It is shown that mechanically stable high conductivity PEO: NH_4I films with high NH_4^+/EO ratios (≥ 0.13), which could not be obtained otherwise, can be obtained by dispersal of α-Al_2O_3 in the host matrix. The addition of α-Al_2O_3 changes the crystallinity and polymer matrix crystallite size and hence the conductivity. The conductivity also depends upon Al_2O_3 content and its particle size.

Acknowledgements

The authors wish to thank Dr D. Pandey for XRD linewidth studies and helpful discussions. Thanks are also due to Ms Neelam Singh for co-operation. One of us (AC) wishes to acknowledge CSIR, New Delhi for the award of a Senior Research Fellowship.

References

1. M. STAINER, L. C. HARDY, D. H. WHITMORE and D. F. SHRIVER, *J. Electrochem. Soc.* **131** (1984) 784.
2. M. F. DANIEL, B. DESBAT and J. C. LASSEGUES, *Solid State Ionics* **28–30** (1988) 632.
3. S. CHANDRA, S. A. HASHMI and G. PRASAD, *ibid.* **40/41** (1990) 651.
4. S. A. HASHMI, A. KUMAR, K. K. MAURYA and S. CHANDRA, *J. Phys. D: Appl. Phys.* **23** (1990) 1307.
5. P. DONSO, W. GORECKI, C. BERTHEIR, F. DEFENDINI, C. POINSIGNORE and M. B. ARMAND, *Solid State Ionics* **28–30** (1988) 969.
6. K. K. MAURYA, S. A. HASHMI and S. CHANDRA, *J. Phys. Soc. Japan* **61** (1992) 1709.
7. K. K. MAURYA, N. SRIVASTAVA, S. A. HASHMI and S. CHANDRA, *J. Mater. Sci.* **27** (1992) 6357.
8. K. SHAHI and J. B. WAGNER, *Solid State Ionics*, **3/4** (1981) 295.
9. F. CORCE, F. BONINO, S. PANERO and B. SCROSATI, *Phil. Mag. B* **59** (1989) 161.
10. F. W. POULSEN, N. H. KINDL, B. KINDL and J. SCHOONMAN, *Solid State Ionics* **9–10** (1983) 119.

Received 28 March 1994
and accepted 20 January 1995